Tunnelling Effects of Solitons in Optical Fibers with Higher-Order Effects

Chao-Qing Dai[a,b], Hai-Ping Zhu[c], and Chun-Long Zheng[d]

[a] School of Sciences, Zhejiang A&F University, Lin'an, Zhejiang, 311300, China
[b] School of Physical Science and Technology, Suzhou University, Suzhou, Jiangsu, 215006, China
[c] School of Science, Zhejiang Lishui University, Lishui, Zhejiang, 323000, China
[d] College of Physics and Electromechanical Engineering, Shaoguan University, Guangdong 512005, China

Reprint requests to C.-Q. D.; E-mail: dcq424@126.com

Z. Naturforsch. **67a,** 338 – 346 (2012) / DOI: 10.5560/ZNA.2012-0033
Received October 18, 2011 / revised January 10, 2012

We construct four types of analytical soliton solutions for the higher-order nonlinear Schrödinger equation with distributed coefficients. These solutions include bright solitons, dark solitons, combined solitons, and M-shaped solitons. Moreover, the explicit functions which describe the evolution of the width, peak, and phase are discussed exactly. We finally discuss the nonlinear soliton tunnelling effect for four types of femtosecond solitons.

Key words: Nonlinear Schrödinger Equation; Higher-Order Effect; Soliton Solutions; Tunnelling Effect.
PACS numbers: 05.45.Yv; 42.65.Tg

1. Introduction

During the past few decades, terrestrial and submarine communication systems have scored an incredible growth of their transmission capacity. Optical solitons have been witnessed as good information carriers for long distance communication and all-optical ultrafast switching devices. The standard nonlinear Schrödinger equation (NLSE), as an important physical model, describes the dynamics of picosecond optical soliton propagation in nonlinear optical fibers [1], where soliton formation is an interplay between group-velocity dispersion (GVD) and self-phase modulation (SPM). When short pulses are considered (to nearly 50 fs), we should consider the third-order dispersion (TOD) which will produce an asymmetrical broadening in the time domain for the ultrashort soliton pulses [2]. Moreover, the higher-order nonlinear effects such as the self-steepening (SS) and self-frequency shift (SFS) etc. cannot be neglected. The SS, otherwise called the Kerr dispersion, is due to the intensity dependence of the group velocity. This forces the peak of the pulse to travel slower than the wings, which causes an asymmetrical spectral broadening of the pulse [3]. The SFS due to stimulated Raman scattering results in an increasing redshift in the pulse spectrum, in which the long wavelength components experience Raman gain at the expense of the short wavelength components [4]. It has been recognized that the SFS is a potentially detrimental effect in soliton communication systems [5]. Thus the propagation of femtosecond optical pulses can be described by the higher-order nonlinear Schrödinger equation (HNLSE) [6].

In a real fiber, the core medium is inhomogeneous [7]. There will always be some nonuniformity due to many factors and important among them are (i) that which arises from a variation in the lattice parameters of the fiber medium, so that the distance between two neighbouring atoms is not constant throughout the fiber, (ii) that which arises due to the variation of the fiber geometry (diameter fluctuations, and so on). These nonuniformities influence various effects such as loss (or gain), dispersion, phase modulation, SS and SFS etc. and lead to the variable coefficients in the NLSE. Moreover, the variable-coefficient NLSEs have attracted a great deal of interest in dispersion-managed optical fibers [8 – 17]. Picosecond soliton control, described by the variable-coefficient (vc) NLSE, has been extensively studied theoretically [8 – 13]. More recently, studies of fem-

tosecond soliton control, described by the vcHNLSE, have been developed [14 – 17].

From the canonical presentation of quantum tunnelling, when the maximum of the potential barrier is larger than the energy of the point-like particle, the Schrödinger equation allows non-vanishing wave functions in the classically forbidden region on the other side of the barrier. Similarly, when a soliton (as a quasi-particle) propagates towards a finite potential barrier (depending only on the spatial coordinate), the soliton can tunnel through the barrier in a lossless manner [18]. Historically, the study of soliton tunnelling effects governed by the vcNLSE began with the pioneering work of Serkin and Belyaeva [19] since Newell predicted the tunnelling effect in 1978 [18] which exists in nonlinear media. Subsequently, the tunnelling effects of solitons governed by various vcNLSE were extensively discussed. For instance, Wang et al. [20] discussed the tunnelling effects of spatial similaritons passing through a nonlinear barrier (or well). Dai et al. [21, 22] studied the tunnelling effects of bright and dark similaritons in the birefringent fiber. Recently, Segev and collaborators [23] discovered experimentally the nonlinear spatial soliton tunnelling effects of a paraxial Gaussian beam launched in a trap potential. By increasing the power levels, the dynamics transformed from linear tunnelling to nonlinear tunnelling, and then to a narrow spatial soliton ejection. More recently, enigmas of optical and matter-wave soliton nonlinear tunnelling has also been uncovered in [24].

Recently, many authors discussed $(1+1)$-dimensional [25 – 28], $(2+1)$-dimensional [29], and $(3+1)$-dimensional [30] vcNLSEs. However, the nonlinear tunnelling effects for femtosecond solitons have been hardly investigated until now except that Porsezian et al. [31] discussed the in-phase injection interaction through a dispersion barrier (DB). Thus, some interesting issues arise: Whether can optical solitons be controlled in the femtosecond regime? What does happen when femtosecond solitons, such as bright solitons, dark solitons, and combined W-shaped and M-shaped solitons, pass through a DB/dispersion well (DW) or TOD barrier (TODB)/well (TODW)? To answer these problems, we consider the vcHNLSE as follows [17]:

$$\begin{aligned} &\mathrm{i}u_z + a(z)u_{tt} + b(z)|u|^2u + \mathrm{i}c(z)u_{ttt} + \mathrm{i}d(z)(|u|^2u)_t \\ &+ \mathrm{i}e(z)u(|u|^2)_t + \mathrm{i}f(z)u_t + [g(z) + yh(z)]u = 0\,, \end{aligned} \tag{1}$$

where $u(z,t)$ is the complex envelope of the electrical field, z and t, respectively, represent the propagation distance and retarded time, while all the variable coefficients are real analytical functions. $a(z)$ and $c(z)$ represent group-velocity dispersion and TOD, respectively. $b(z)$ is the nonlinearity parameter induced SPM, the parameters $d(z)$ and $e(z)$ are, respectively, related to SS and SFS. The term proportional to $f(z)$ results from the group velocity, $g(z)$ denotes the external electro-optic phase modulation, and $h(z)$ represents the attenuation or absorption coefficient. When $f(z) = g(z) = 0$, (1) can be extensively used to describe the telecommunication and ultrafast signal-routing systems in the weakly dispersive and nonlinear dielectrics with distributed parameters [12, 14, 16, 17]. If the higher-order terms are neglected [i.e. $c(z) = d(z) = e(z) = 0$], (1) degenerates to the vcNLSE [32]. If $c(z) = e(z) = 0$, (1) reduces to the derivative vcNLSE [33], which describes the optical soliton propagation in the presence of Kerr dispersion.

2. Reduction Procedure

In order to get the exact analytical solutions for (1), we construct the mapping transformation

$$u(z,t) = A(z)E[T(z,t),Z(z)]\exp[\mathrm{i}\phi(z,t)]\,, \tag{2}$$

where the amplitude $A(z)$ and the phase $\phi(z,t)$ are real functions, $E \equiv E(T,Z), T \equiv T(z,t)$, and $Z \equiv Z(z)$ are two real functions to be determined. Then the vcHNLSE (1) is transformed into the constant-coefficient (cc) HNLSE [5, 34 – 36]

$$\begin{aligned} E_Z = \mathrm{i}(&\alpha_1 E_{TT} + \alpha_2|E|^2E) + \alpha_3 E_{TTT} \\ &+ \alpha_4(|E|^2E)_T + \alpha_5 E(|E|^2)_T = 0\,. \end{aligned} \tag{3}$$

The substitution of (2) into (1) leads to (3), but now we must have

$$A_z + hA - 3cA\phi_t\phi_{tt} + aA\phi_{tt} = 0\,, \tag{4}$$

$$T_z + 2aT_t\phi_t - 3cT_t\phi_t^2 + fT_t = 0\,, \tag{5}$$

$$\phi_z + a\phi_t^2 + c\phi_{ttt} - c\phi_t^3 + f\phi_t + g = 0\,, \tag{6}$$

$$cT_t\phi_{tt} = 0\,,\ \ T_{tt} = 0\,, \tag{7}$$

$$(b - d\phi_t)A^2 = \alpha_2 Z_z\,,\ \ (a - 3c\phi_t)T_t^2 = \alpha_1 Z_z\,, \tag{8}$$

$$\begin{aligned} &cT_t^3 + \alpha_3 Z_z = 0\,,\ \ eA^2T_t + \alpha_5 Z_z = 0, \\ &dA^2T_t + \alpha_4 Z_z = 0\,. \end{aligned} \tag{9}$$

Solving the set of partial differential equations (4)–(9), we obtain the mapping variable T, the effective propagation distance Z, the amplitude A, and the phase ϕ of the pulse as

$$T = k\left[t + p\left(\frac{2k\alpha_1}{\alpha_3} - 3p\right)\int_0^z c(s)\,\mathrm{d}s - \int_0^z f(s)\,\mathrm{d}s\right] + t_0\,, \tag{10}$$

$$Z = -\frac{k^3}{\alpha_3}\int_0^z c(s)\,\mathrm{d}s\,, \tag{11}$$

$$A = A_0 \exp\left[-\int_0^z h(s)\,\mathrm{d}s\right], \tag{12}$$

$$\phi = p\left[t + p\left(\frac{k\alpha_1}{\alpha_3} - 2py\right)\int_0^z c(s)\,\mathrm{d}s - \int_0^z f(s)\,\mathrm{d}s\right] + \int_0^z g(s)\,\mathrm{d}s + \phi_0\,. \tag{13}$$

Note that the parameters k and p are related to pulse width and phase shift, respectively. The TOD parameter $c(z)$ influences the form of the phase and the effective propagation distance. Also note that the mapping transformation (3) has been applied to the vcNLSE in [37, 38]; however, its application to the vcHNLSE is relatively less reported. Compared with the corresponding solutions in [39], a control parameter $f(z)$ is added in our solutions (10) and (13), which make our results more coincident with the real situation. Also note that the added parameter $f(z)$ in solutions (10) and (13) can not be transformed by $t = t - fz$, which used to change (1) with constant coefficients into the corresponding equation in [39] with constant coefficients.

Further, the constraints of system parameters are given as

$$c(z) : a(z) : b(z) : d(z) : e(z) = 1 : \left(3p - \frac{k\alpha_1}{\alpha_3}\right) : \frac{k^2(p\alpha_4 - k\alpha_2)}{\alpha_3 A_0^2}\exp\left[2\int_0^z h(s)\,\mathrm{d}s\right] : \frac{k^2\alpha_4}{A_0^2\alpha_3}\exp\left[2\int_0^z h(s)\,\mathrm{d}s\right] : \frac{k^2\alpha_5}{A_0^2\alpha_3}\exp\left[2\int_0^z h(s)\,\mathrm{d}s\right]. \tag{14}$$

Thus, the substitution

$$u = A_0 E\left\{k\left[t + p\left(\frac{2k\alpha_1}{\alpha_3} - 3p\right)\int_0^z c(s)\,\mathrm{d}s - \int_0^z f(s)\,\mathrm{d}s\right] + t_0,\ -\frac{k^3}{\alpha_3}\int_0^z c(s)\,\mathrm{d}s\right\}\exp\left[-\int_0^z h(s)\,\mathrm{d}s + \mathrm{i}\phi\right], \tag{15}$$

where ϕ satisfies (13), leads to (2) with the condition (14). The solutions of (1) can be obtained from those of (2) via the transformation (15).

The one-to-one correspondence (15) admits us to obtain abundant solutions, such as bright and dark soliton solutions, W-shaped and M-shaped soliton solutions, and so on.

3. Tunnelling Effects of Bright and Dark Solitons

Employing the transformation (15) and the Darboux transformation (DT) method [16], and when $\alpha_4 = -\alpha_5, 3\alpha_2\alpha_3 = \alpha_1\alpha_4$, one can obtain bright multi-solitons for (1):

$$u = A(z)\,\mathrm{e}^{\mathrm{i}\phi(z,t)} \cdot \left[u_0 + 2\sqrt{\frac{2\alpha_1}{\alpha_2}}\sum_{m=1}^{n}\frac{(\lambda_m + \lambda_m^*)\varphi_{1,m}(\lambda_m)\varphi_{2,m}^*(\lambda_m)}{A_m}\right], \tag{16}$$

with

$$\begin{aligned}\varphi_{j,m+1}(\lambda_{m+1}) &= (\lambda_{m+1} + \lambda_m^*)\varphi_{j,m}(\lambda_{m+1}) - \frac{B_m}{A_m}(\lambda_m + \lambda_m^*)\varphi_{j,m}(\lambda_m)\,,\\ A_m &= |\varphi_{1,m}(\lambda_m)|^2 + |\varphi_{2,m}(\lambda_m)|^2,\\ B_m &= \varphi_{1,m}(\lambda_{m+1})\varphi_{1,m}^*(\lambda_m) + \varphi_{2,m}(\lambda_{m+1})\varphi_{2,m}^*(\lambda_m)\,,\end{aligned} \tag{17}$$

where DT times $m = 1,\ldots,n$, $j = 1,2$, complex spectral parameters $\lambda_m = \frac{1}{2}(\eta_m + \mathrm{i}\xi_m)$, λ_m^* is the complex conjugate of λ_m, $T, Z, A(z)$, and $\phi(z,t)$ satisfy (10)–(13). $(\varphi_{1,1}(\lambda_1), \varphi_{2,1}(\lambda_1))^{\mathrm{T}}$ is the eigenfunction corresponding to λ_1 for u_0, and $\varphi_{j,1} = \exp\left(\frac{\delta_j}{2} + \mathrm{i}\frac{\kappa_j}{2}\right)$ with

$$\begin{aligned}\delta_j &= \eta_j\left[T + \left(\eta_j^2 - 3\xi_j^2\right)\alpha_3 Z - 2\xi_j\alpha_1 Z\right] - \delta_{j0}\,,\\ \kappa_j &= \xi_j T + \xi_j\left(3\eta_j^2 - \xi_j^2\right)\alpha_3 Z + \left(\eta_j^2 - \xi_j^2\right)\alpha_1 Z - \kappa_{j0}\,.\end{aligned} \tag{18}$$

Inserting the zero seeding solution of (1) as $u_0 = 0$ into (16), one can obtain a one-soliton solution for (2). Using that one-soliton solution as the seed solution in (16), we can obtain two-soliton solutions. Thus in recursion, one can generate up to n-solitons solutions. Here we present bright one- and two-solitons in explicit forms. The one-soliton reads

$$u = \sqrt{2\alpha_1/\alpha_2}\,\eta_1 A(z)\,\mathrm{sech}\delta_1 \cdot \exp\{\mathrm{i}[\phi(z,t) + \kappa_1(Z,T)]\}\,, \tag{19}$$

where δ_1 and κ_1 are given by (12). The analytical bright soliton pairs reads

$$u = \sqrt{2\alpha_1/\alpha_2}A(z)\,\mathrm{e}^{\mathrm{i}\phi(z,t)}G_1/F_1\,, \tag{20}$$

where $G_1 = a_1\cosh\delta_2\,\mathrm{e}^{\mathrm{i}\kappa_1} + a_2\cosh\delta_1\,\mathrm{e}^{\mathrm{i}\kappa_2} + \mathrm{i}a_3(\sinh\delta_2\,\mathrm{e}^{\mathrm{i}\kappa_1} - \sinh\delta_1\,\mathrm{e}^{\mathrm{i}\kappa_2})$, $F_1 = b_1\cosh(\delta_1+\delta_2) + b_2\cosh(\delta_1-\delta_2) + b_3\cos(\kappa_2-\kappa_1)$, $a_j = \frac{\eta_j}{2}\left[\eta_j^2 - \eta_{3-j}^2 + (\xi_1-\xi_2)^2\right]$, $b_j = \frac{1}{4}\left\{\left[\eta_1+(-1)^j\eta_2\right]^2 + (\xi_1-\xi_2)^2\right\}$, $a_3 = \eta_1\eta_2(\xi_1-\xi_2)$, and $b_3 = -\eta_1\eta_2$, $j = 1,2$. δ_j and κ_j are given by (18).

Similarly, based on solutions of the ccHNLSE [33], one can also derive dark (grey) multi-solitons for (1). For simplicity, here we only present dark (grey) one- and two-soliton solutions in explicit forms. The exact grey soliton pairs read

$$u = \mu\sqrt{-2\alpha_1/\alpha_2}A(z)\,\mathrm{e}^{\mathrm{i}[\phi(z,t)+\varphi(Z,T)]} \cdot (1+G_2/F_2)\,, \tag{21}$$

where $G_2 = 4\mu(\omega_1+\omega_2-2\mu) - 4\mathrm{i}\frac{\lambda_1+\lambda_2}{\eta_1+\eta_2}\rho$, $F_2 = 4\mu^2 + \left(\frac{\lambda_1+\lambda_2}{\eta_1+\eta_2}\right)^2\rho$, $\rho = (\omega_1-\mu)(\omega_2-\mu)$, $\omega_j = (\xi_j - \mathrm{i}\eta_j)[\xi_j + \mathrm{i}\eta_j\tanh(\delta_j)]/\mu$, $\delta_j = \eta_j\left[T - T_{j0} - \left(2\eta_j^2 + 3\xi_j\right)\alpha_3 Z + 2\xi_j\alpha_1 Z\right]$, $\varphi(Z,T) = \xi_j T - \xi_j\left(6\eta_j^2 + \xi_j^2\right)\alpha_3 Z + \left(2\eta_j^2 + \xi_j^2\right)\alpha_1 Z - \varphi_0$, $\lambda_j = \xi_j + \mathrm{i}\eta_j$, and $\mu = |\lambda_j|, j = 1,2$. And the exact dark one soliton reads

$$u = \sqrt{\frac{-2\alpha_1}{\alpha_2}}\frac{\xi_1 - \mathrm{i}\eta_1}{\mu}A(z)[\xi_1 + \mathrm{i}\eta_1\tanh(\delta_1)] \cdot \mathrm{e}^{\mathrm{i}[\phi(z,t)+\varphi(Z,T)]}. \tag{22}$$

From the relation (14), if $h = 0$, then $b(z) : a(z) = k^2(p\alpha_4 - k\alpha_2) : A_0^2(3\alpha_3 p - k\alpha_1) = \text{const}$. If h is a function of z, then $h = (b_z a - a_z b)/(2ab)$, which is identical with the condition expressed as (7) in [17, 31]. Under this constraint some properties such as the multi-soliton solutions have been discussed by the auto-Bäcklund transformation and Darboux transformation method [17, 31]. To our knowledge, the investigation of (1) under constraints (14) has not been widespread.

Note that soliton-pairs through DB have been discussed under the integrable condition $h = (b_z a - a_z b)/(2ab)$ [31], where the pulses are amplified and form the peaks, then attenuate and recover their original shape. Similar to picosecond pulses [21, 22], when femtosecond pulses pass through DW, the pulses' amplitudes diminish, form the dips, then attenuate and increase their amplitudes. For the limit of length, we omit these discussions. Here we focus on two other interesting cases as follows.

Firstly, due to the existence of function $f(z)$, we can modulate the behaviours of solitons passing through TODB or TODW with $c(z) = 1 + \delta\,\mathrm{sech}^2[\sigma(z-z_0)]$, where δ represents the barrier's amplitude, whose positive or negative sign denotes the barrier or the well. As $c(z) > 0$, we assume $\delta > -1$, where $\delta > 1$ indicates the TODB, and $-1 < \delta < 0$ represents the TODW. σ is the parameter relating to the barrier's width, and z_0 represents the longitudinal coordinate indicating the location of barrier (or well). From Figures 1 and 2, when bright soliton pairs going through TODB and TODW, peaks and dips are formed, respectively. Moreover, function $f(z)$ adds the appearance domain of TODB or TODW seen from Figures 1b, 2b, and 2d. Specially, if the emerging distance of the well coincides with that of interaction, the wells in Figures 2c and 2d decrease the level of interaction comparing with the case in Figures 2a and 2b. This presents a potentially important method for fading the hazard of soliton interaction in optical fiber, and it is also significant to increase the information bit rate or decrease the bit-error-rate in the optical soliton communications. Figure 3 displays

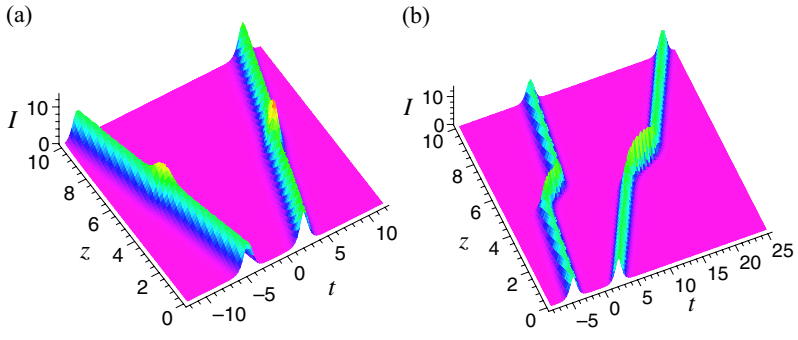

Fig. 1 (colour online). Separated bright soliton pairs going through TODB with (a) $f = 0$ and (b) $f = 1 + 5\,\mathrm{sech}^2[3(z-z_0)]$. The parameters are $A_0 = t_0 = k = -p = 1$, $\delta = 0.5$, $\sigma = 2$, $z_0 = 5$, $\alpha_1 = \alpha_3 = 2$, $\alpha_2 = 1$, $\alpha_4 = 3$, $\xi_1 = \eta_2 = 1.4$, $\xi_2 = \eta_1 = 1.5$, $\delta_{10} = -\delta_{20} = 2$, $\kappa_{10} = \kappa_{20} = 1$.

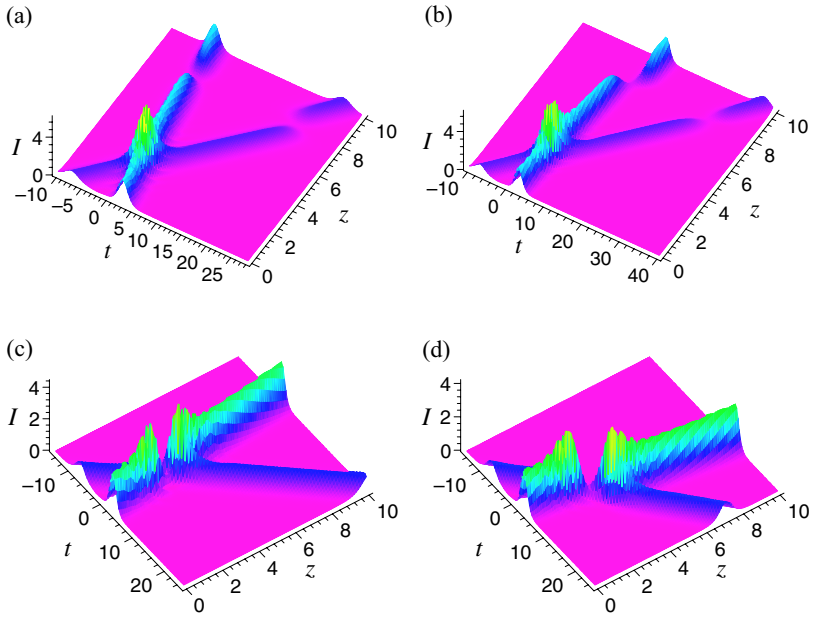

Fig. 2 (colour online). Interacting bright soliton pairs going through TODW with (a),(c) $f = 0$ and (b),(d) $f = 1+5\mathrm{sech}^2[3(z-z_0)]$. The parameters are $A_0 = t_0 = k = -p = 1$, $\delta = -0.9$, $\sigma = 1.6$, $\alpha_1 = \alpha_3 = 2$, $\alpha_2 = 1$, $\alpha_4 = 3$, $\eta_1 = 0.5$, $\eta_2 = 0.8$, $\xi_1 = -\xi_2 = -1$, $\delta_{10} = -\delta_{20} = -3$, $\kappa_{10} = \kappa_{20} = 1$ with (a),(b) $z_0 = 8$ and (c),(d) $z_0 = 3$.

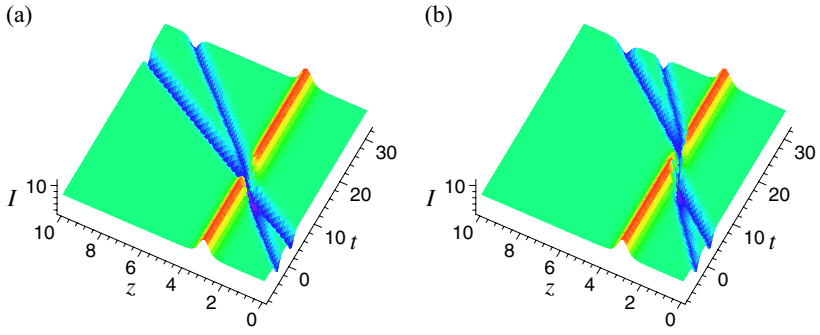

Fig. 3 (colour online). Interacting dark soliton pairs going through TODB with (a) $f = 0$ and (b) $f = 1 + 5\mathrm{sech}^2[3(z - z_0)]$. The parameters are $A_0 = t_0 = k = -p = 1$, $\delta = 0.8$, $\sigma = 3$, $z_0 = 3$, $\alpha_1 = \alpha_3 = -2$, $\alpha_2 = 1$, $\alpha_4 = 3$, $T_{10} = -T_{20} = -2.5$, $\eta_1 = \eta_2 = 1$, $\xi_1 = -\xi_2 = -0.8$.

interacting dark soliton pairs passing through TODB. When a dark soliton pair passes through the barrier, a wall appears near $z = z_0$ in Figure 3. Similarly, comparing Figure 3a with Figure 3b, we find that function $f(z)$ adds the appearance domain of TODB and produces a position shift after passing the barrier for the dark soliton case.

As second example, we discuss soliton behaviours for $h = 0$ and $b(z)$ satisfying the expression of DB or DW with $b(z) = 1 + \delta\mathrm{sech}^2[\sigma(z - z_0)]$. An interesting phenomenon is shown in Figure 4a. A tunnelling effect between separated soliton pairs going through the DB is found, and the energy of the two solitons exchanges at the location of the barrier with $z = z_0 = 5$. The energy of the left soliton changes from small to large after passing through the DB, and the opposite case appears in the right soliton. From Figure 4b, we have not found the tunnelling effect between separated soliton pairs.

Historically, the first demonstration that the soliton is a composite particle possessing an inner degree of freedom was found by Kosevich [40]. This physical mechanism of the soliton decay during its scattering is hereafter referred to as the Kosevich mechanism of soliton decay. Nonlinear soliton behaviour differs essentially from quantum mechanical linear tunnelling, and in particular, from Figures 1 – 4, we have found the possibility for solitons to propagate with sudden and full transmission corresponding to the observed soliton ejection in [41]. This phenomenon is similar to the cor-

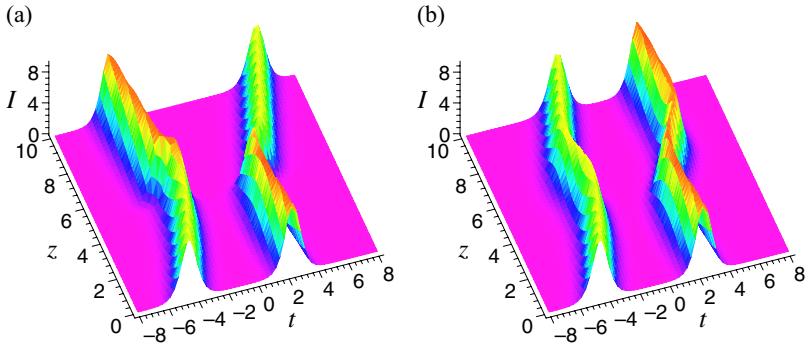

Fig. 4 (colour online). Tunneling effect between separated bright soliton pairs going through (a) DB with $\delta = 8$, $\sigma = 5$ and (b) DW with $\delta = -3$, $\sigma = 0.8$ under system parameter $f = 0.2$, $h = 0$. Other parameters are the same as that in Figure 1.

responding case in [24], where authors have reported that increasing of the soliton binding energy (similar to the nuclear binding energy) enables the testing of a long-standing theoretical result that predicts that an optical soliton can tunnel between two regions of anomalous dispersion across a forbidden region of normal dispersion (enhanced soliton spectral tunnelling effect).

4. Tunnelling Effects of Combined Solitons

By assuming an imaginary amplitude for the ccHNLSE in [35, 36], W-shaped solitons and M-shaped solitons are discussed. Moreover, we also investigated W-shaped and M-shaped solitons for the vcHNLSE [42] by imaginary amplitude. Here we obtain combined bright and dark solitons, W-shaped solitons, and M-shaped solitons by assuming a real amplitude based on the direct ansatz method. It is worthwhile to note that we here derive these solitary wave solutions, including bright and dark combined solitons, W-shaped and M-shaped solitons, by assuming a real amplitude instead of assuming an imaginary amplitude in [42, 43]. We make the ansatz for (1) as $u(z,t) = v(z,t)\exp[\mathrm{i}\varphi(z,t)]$ with the real function $v(z,t) = a_0(z) + a_1(z)\mathrm{sech}(\xi) + b_1(z)\tanh(\xi)$, or $v(z,t) = a_0(z) + a_1(z)\mathrm{sech}(\xi)\tanh(\zeta)$, where $\xi(z,t) = p(z)t + q(z)$, $\zeta = m(z)t + q(z)$, $\varphi(z,t) = \Gamma(z)t + \Omega(z)$, and then substituting them into (1). When $a(z) = c(z) = 0$, $3d(z) + 2e(z) = 0$, $b(z) = \Gamma_0 d(z)$, we derive bright and dark combined solitons and M-shaped solitons in the forms

$$u(z,t) = \{A_1 + A_2\mathrm{sech}[P\theta(z,t)] + B_1\tanh[P\theta(z,t)]\} \cdot \exp\left[\mathrm{i}\varphi(z,t) - \int_0^z h(z)\,\mathrm{d}z\right] \tag{23}$$

and

$$u(z,t) = A_3\tanh[P\theta(z,t)]\mathrm{sech}[Q\theta(z,t)] \cdot \exp\left[\mathrm{i}\varphi(z,t) - \int_0^z h(z)\,\mathrm{d}z\right], \tag{24}$$

where

$$\theta(z,t) = t - \int_0^z f(z)\,\mathrm{d}z, \varphi(z,t) = \Gamma_0\left\{t - \int_0^z [g(z) + \Gamma_0 f(z)]\,\mathrm{d}z\right\}, \tag{25}$$

with real constants A_1, A_2, B_1, A_3, P, Q, and Γ_0. Note that the term proportional to $f(z)$ resulting from the group velocity is very important because it determines the group velocity and the phase shift of these solitons.

Next we discuss tunnelling effects of combined solitons. From solutions (23)–(25), one knows that the group velocity and the phase shift are decided by $f(z)$, and the amplitude of the solitary wave depends on the gain or loss coefficient $h(z)$. This combined soliton (23) can describe the properties of both bright and dark solitons, and its amplitude does not approach zero when the time variable approaches infinity unless it changes into the kink solitary wave. This solitary wave depends on its coefficient A_2 and B_1 relations. Especially, if $B_1 = 0$ and $A_1A_2 < 0$, $|A_2| > |A_1|$, we can obtain a W-shaped soliton, which might be one of the possible explanations for a single soliton-like pulse shape with a pronounced platform underneath it as commented by Bullough attached to [43]. From Figures 5 and 6, when combined solitons and W-shaped solitons go through TODB and TODW, the walls and channels appear, respectively. Obviously, the propagation characteristic of these combined solitons passing through TODB and TODW is similar to that of the

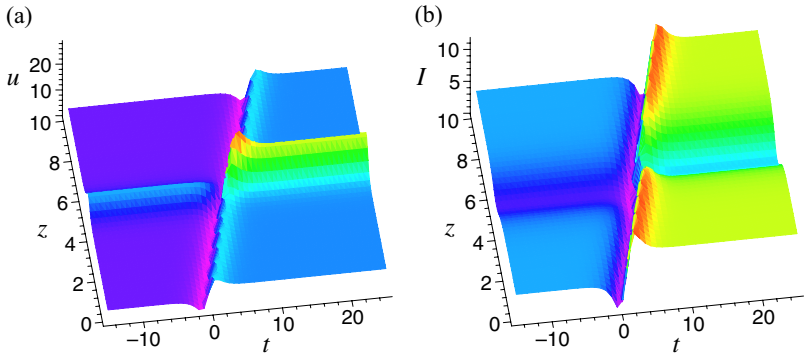

Fig. 5 (colour online). Combined solitons passing through TODB with $\delta = 1.5$, $\sigma = 2$ and through TODW with $\delta = -0.5$, $\sigma = 1$. The parameters are $A_1 = 0.5$, $A_2 = 1.5$, $B_1 = 2.5$, $P = 1$, $Q = 2$, $z_0 = 5$.

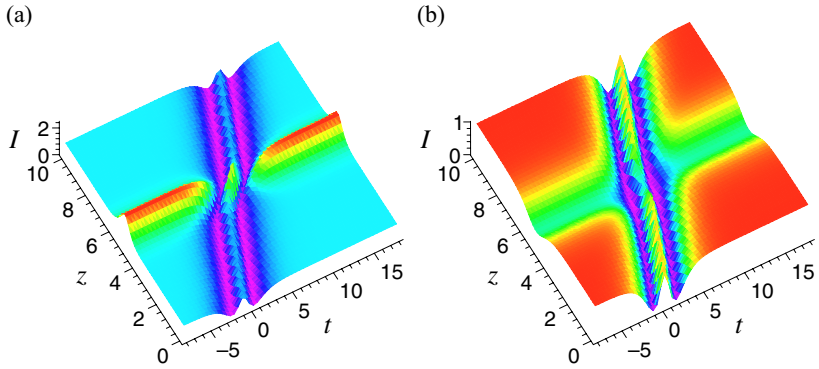

Fig. 6 (colour online). W-shaped solitons passing through TODB with $\delta = 1.5$, $\sigma = 2$ and through TODW with $\delta = -0.5$, $\sigma = 1$. The parameters are $A_1 = 1$, $A_2 = -2$, $B_1 = 0$, $P = 1$, $Q = 2$, $z_0 = 5$.

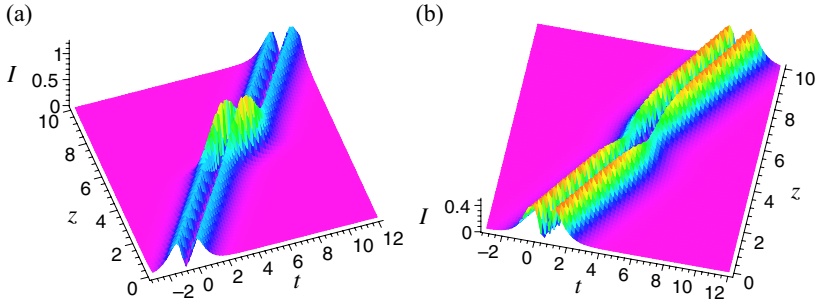

Fig. 7 (colour online). M-shaped solitons passing through TODB with $\delta = 1.5$, $\sigma = 2$ and through TODW with $\delta = -0.5$, $\sigma = 1$. The parameters are $A_2 = P = 1$, $z_0 = 5$.

dark soliton pairs shown in Figure 3. It is well known that a M-shaped soliton might be one of the possible models for a femtosecond dark pulse transmission with finite width background bright pulse. Therefore, it is significant that the investigation to M-shaped solitons has a share in understanding femtosecond dark pulse transmission. As shown in Figure 7, when a M-shaped soliton passes through TODB and TODW, the peaks and dips are produced, respectively, which is not similar to the corresponding case of dark soliton pairs in Figure 3, but that of bright soliton pairs in Figures 1 and 2.

5. Conclusions

In conclusion, we have constructed the relation between the vcHNLSE describing the femtosecond pulse propagation and the ccHNLSE via a transformation. Based on this transformation, we analytically obtained bright and dark solitons for the vcHNLSE. More-

over, we obtain combined bright and dark solitons, W-shaped solitons, and M-shaped solitons by assuming a real amplitude based on the direct ansatz method. Then based on these solutions, we discuss tunnelling effects for four types of femtosecond solitons. When bright solitons, combined solitons, and W-shaped solitons pass through the barrier and well, peaks and dips are form, respectively. When dark solitons and M-shaped solitons go through the barrier and well, walls and channels appear, respectively. Moreover, we discuss the role of the term proportional to $f(z)$ from the group velocity for tunnelling effect. The tunnelling effect between separated bright soliton pairs is also studied. Of course, due to the lack of an experimental and designed basis related to these theoretical results, we could not give further details about the real physical application. We expect that these results for femtosecond soliton tunnelling would inaugurate a new and exciting area in the application of optical solitons.

Acknowledgements

This work was supported by the National Natural Science Foundation of China (Grant Nos. 11005092 and 11172181), the Program for Innovative Research Team of Young Teachers (Grant No. 2009RC01), and the Scientific Research and Developed Fund (Grant No. 2009FK42) of Zhejiang A&F University.

[1] H. A. Haus and W. S. Wong, Rev. Mod. Phys. **68**, 423 (1996).
[2] E. Bourkoff, W. Zhao, R. I. Joseph, and D. N. Christodoulides, Opt. Lett. **12**, 272 (1987).
[3] J. R. de Oliveria, Phys. Rev. E **57**, 4571 (1998).
[4] F. M. Mitschke and L. F. Mollenauer, Opt. Lett. **11**, 657 (1986).
[5] K. Porsezian and K. Nakkeeran, Phys. Rev. Lett. **76**, 3955 (1996).
[6] Y. Kodama, J. Stat. Phys. **39**, 597 (1985).
[7] F. Abdullaeev, Theory of Solitons in Inhomogeneous Media, Wiley, New York 1994.
[8] W. J. Liu, B. Tian, T. Xu, K. Sun, and Y. Jiang, Ann. Phys. (NY) **325**, 1633 (2010).
[9] H. Q. Zhang, B. G. Zhai, and X. L. Wang, Phys. Scr. **85**, 015007 (2012).
[10] C. Q. Dai, Y. Y. Wang, Q. Tian, and J. F. Zhang, Ann. Phys. (NY) **327**, 512 (2012).
[11] C. Q. Dai, D. S. Wang, L. L. Wang, J. F. Zhang, and W. M. Liu, Ann. Phys. (NY) **326**, 2356 (2011).
[12] X. J. Lai and X. O. Cai, Z. Naturforsch. **66a**, 392 (2011).
[13] D. S. Wang and Y. Liu, Z. Naturforsch. **65a**, 71 (2010).
[14] J. F. Zhang, Q. Yang, and C. Q. Dai, Opt. Commun. **248**, 257 (2005).
[15] C. Q. Dai, G. Q. Zhou, and J. F. Zhang, Phys. Rev. E **85**, 016603 (2012).
[16] L. Li, Z. H. Li, S. Q. Li, and G. S. Zhou, Opt. Commun. **234**, 169 (2004).
[17] J. Li, H. Q. Zhang, T. Xu, Y. X. Zhang, and B. Tian, J. Phys. A: Math. Theor. **40**, 13299 (2007).
[18] A. C. Newell, J. Math. Phys. **19**, 1126 (1978).
[19] V. N. Serkin and T. L. Belyaeva, JETP Lett. **74**, 573 (2001).
[20] J. F. Wang, L. Li, and S. T. Jia, J. Opt. Soc. Am. B **25**, 1254 (2008).
[21] C. Q. Dai, Y. Y. Wang, and J. F. Zhang, Opt. Express **18**, 17548 (2010).
[22] C. Q. Dai, R. P. Chen, and J. F. Zhang, Chaos Soliton. Fract. **44**, 862 (2011).
[23] A. Barak, O. Peleg, C. Stucchio, A. Soffer, and M. Segev, Phys. Rev. Lett. **100**, 153901 (2008).
[24] T. L. Belyaeva, V. N. Serkin, C. Hernandez-Tenorio, and F. Garcia-Santibanez, J. Mod. Opt. **57**, 1087 (2010).
[25] Y. Liu, Y. T. Gao, T. Xu, X. Lu, Z. Y. Sun, X. H. Meng, X. Yu, and X. L. Gai, Z. Naturforsch. **65a**, 291 (2010).
[26] R. Radha and V. R. Kumar, Z. Naturforsch. **65a**, 549 (2010).
[27] J. X. Fei and C. L. Zheng, Z. Naturforsch. **66a**, 1 (2011).
[28] Z. Y. Ma, Z. Naturforsch. **66a**, 500 (2011).
[29] D. S. Wang, X. H. Hu, and W. M. Liu, Phys. Rev. A **82**, 023612 (2010).
[30] Y. X. Chen and X. H. Lu, Commun. Theor. Phys. **55**, 871 (2011).
[31] K. Porsezian, A. Hasegawa, V. N. Serkin, T. L. Belyaeva, and R. Ganapathy, Phys. Lett. A **361**, 504 (2007).
[32] C. Q. Dai, Y. Y. Wang, and J. L. Chen, Opt. Commun. **284**, 3440 (2011).
[33] K. W. Chow, L. P. Yip, and R. J. Grimshaw, Phys. Soc. Jpn. **76**, 074004 (2007).
[34] L. Li, Z. H. Li, Z. Y. Xu, G. S. Zhou, and K. H. Spatschek, Phys. Rev. E **66**, 046616 (2002).
[35] Z. H. Li, L. Li, H. P. Tian, and G. S. Zhou, Phys. Rev. Lett. **84**, 4096 (2000).
[36] J. P. Tian, H. P. Tian, Z. H. Li, L. S. Kang, and G. S. Zhou, Phys. Scr. **67**, 325 (2003).
[37] C. Q. Dai, Y. Y. Wang, and J. F. Zhang, Opt. Lett. **35**, 1437 (2010).
[38] C. Q. Dai, R. P. Chen, and G. Q. Zhou, J. Phys. B: At. Mol. Opt. Phys. **44**, 145401 (2011).

[39] C. Q. Dai, G. Q. Zhou, and J. F. Zhang, Int. J. Mod. Phys. B **21**, 2951 (2007).
[40] A. M. Kosevich, Physica D **41**, 253 (1990).
[41] A. Barak, O. Peleg, C. Stucchio, A. Soffer, and M. Segev, Phys. Rev. Lett. **100**, 153901 (2008).
[42] R. C. Yang, L. Li, R. Y. Hao, Z. H. Li, and G. S. Zhou, Phys. Rev. E **71**, 036616 (2005).
[43] L. F. Mollenauer, Philos. Trans. R. Soc. London A **315**, 437 (1985).